Design and Implementation of a Robust Dual output Forward Converter for Space Application

Sahana J K[1], Dr. Anitha G S[2], T K Nagaraju[3], Bhoopendra Kumar Singh[4]

[1]*P G Student, RV College of Engineering, Bengaluru*
[2]*Associate Professor, RV College of Engineering, Bengaluru*
[3]*Assistant Manager, Centum Electronics Limited, Bengaluru*
[4]*Director, Centum Electronics Limited, Bengaluru*

---***---

Abstract—* *This paper focuses on the design of a forward converter for space application to solve major problems in power management, efficiency, and reliability. The converter uses advanced technology to ensure stable operation in harsh environments. It incorporates key features such as EMI filtering, radiation-hardened components, and thermal management systems to ensure durability in space. It includes a current transformer for sensing, an input under-voltage shutdown for protection, and a feedforward and PWM controller for output regulation. Magnetic Amplifiers and Optocouplers provide additional stability and isolation. Future advancement includes AI-driven control, and cost-effective, eco-friendly designs. Simulation and testing will demonstrate the converter's performance, ensuring it meets the space mission requirements.

Index Terms— EMI, Magnetic Amplifiers, Optocouplers, PWM controller, feedforward.

1. INTRODUCTION

THE design of power supplies is a crucial factor in determining the performance, efficiency, and reliability of modern electronic devices[1]. Among the various power supply configurations, Switched-Mode Power Supplies (SMPS) have gained widespread adoption due to their superior efficiency, compact design, and adaptability to various applications. SMPS technology is utilized in a variety of electronic systems, ranging from consumer electronics to industrial equipment, owing to its ability to convert electrical power with minimal energy loss efficiently [2].

This paper analyzes SMPS architecture in-depth, emphasizing the essential functional blocks contributing to its operation. It outlines the core components, including the Electromagnetic Interference (EMI) filter, rectification and filtering stages, Pulse Width Modulation (PWM) control, and output regulation circuits. The EMI filter is vital in reducing noise emissions, and ensuring compliance with electromagnetic compatibility standards [3]. The rectification and filtering stages transform the AC input into a stable DC output, which is then regulated by control circuits to maintain consistent power delivery under varying load conditions.

A critical aspect of SMPS design is the choice of topology, which can significantly influence the power supply performance. Common SMPS topologies include buck, boost, buck-boost, and flyback configurations, each with unique characteristics suited to different applications. For instance, the buck converter is ideal for stepping down voltage, while the boost converter is used for stepping up voltage.[4] The flyback topology is popular in low to medium power applications due to its simplicity and ability to provide multiple output voltages.

The efficiency and performance of an SMPS are not only determined by the choice of topology but also by the meticulous design of its control and feedback mechanisms [5]. The Pulse Width Modulation (PWM) controller, a cornerstone of SMPS operation, regulates the duty cycle of the switching transistors, thereby controlling the output voltage and current [6]. Advanced PWM techniques, such as current-mode control and voltage-mode control, offer enhanced stability and response times, which are crucial for managing dynamic loads and minimizing ripple [7]. Additionally, the integration of feedforward compensation in the control loop can further improve transient response, making the power supply more resilient to sudden changes in input voltage or load demand. The design and selection of these components are critical, as they directly influence the power density, efficiency, and thermal management of the power supply.[8] By analyzing these factors, the study aims to provide a holistic understanding of the interplay between topology, control strategies, and component design, all of which contribute to the overall effectiveness of SMPS in various applications. A mag amp is a wire coil on a core with a square B-H characteristic. The coil has two operating modes: unsaturated, the core acts as a high inductance, supporting high voltages with minimal current flow. The coil's impedance lowers to near zero when the core saturates, allowing current to flow with little voltage drop.[9]

2. WORKING PRINCIPLE

The forward converter works by isolating the input and transforming its voltage using a transformer so that it can be transferred to the output during the "on" phase of the switching cycle.

Switch On: In the forward converter, a primary-side switch (usually a transistor like a MOSFET) is used to control the flow of current through the primary winding of a transformer The steady DC output is produced when the main switch is turned on by rectifying the induced voltage in the secondary winding with a diode and then filtering it with an output filter. The magnetic amplifier further regulates the secondary output by varying the width of the pulse.

Switch Off: The transformer's magnetic field collapses and the main current stops when the switch is turned off. The primary and secondary windings experience polarity-reversed voltages as a result of this collapse. The reset provides a path for the magnetizing current to dissipate, thereby resetting the core for the next switching cycle.

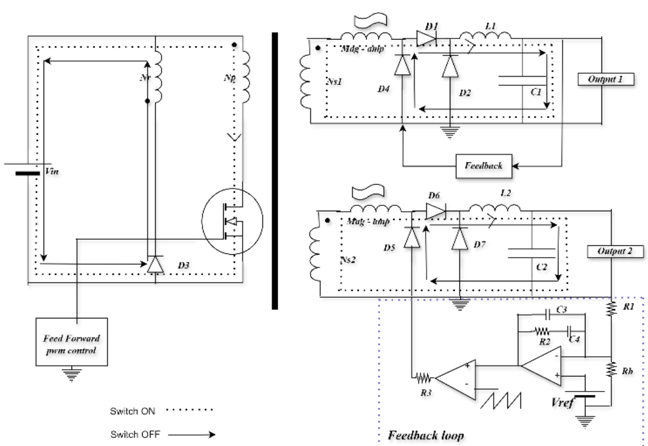

Fig. 1. Forward converter operation

3. METHODOLOGY AND BLOCK DIAGRAM

The sequence to follow any converter after the specification details known

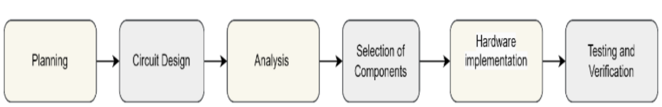

Fig. 2. Steps to design the hardware

The Forward Converter topology is used, and the Input DC bus voltage is adjustable within the range of 30V to 44V. The diagram above illustrates the intricate block design of a Forward Converter with post-regulation based on a Magnetic Amplifier (Mag-Amp). DC-DC Converter is added with an input filter to prevent small AC components from causing performance issues. The primary functions of the filter are to attenuate electrical noise originating from the power source and to mitigate the impact of interference on neighboring devices. The start-up circuit supplies power to the ICs until the bias-winding generates the necessary voltage to initiate the converter. Bias winding is employed to produce the bias voltage required to energize the controller circuits. This voltage is maintained at a greater level than the start-up circuit voltage to ensure that a PWM controller circuit draws current from the bias winding rather than the start-up circuit. The Forward Converter topology is used, and the Input DC bus voltage is adjustable within the range of 30V to 44V.

The diagram above illustrates the intricate block design of a Forward Converter with post-regulation based on a Magnetic Amplifier (Mag-Amp). DC-DC Converter is added with an input filter to prevent small AC components from causing performance issues. The primary functions of the filter are to attenuate electrical noise originating from the power source and to mitigate the impact of interference on neighboring devices.

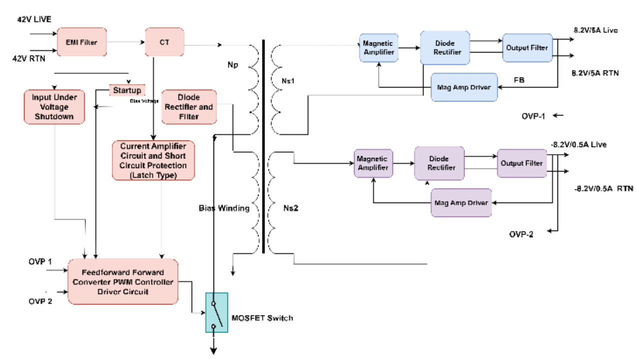

Fig.3 Block diagram of the system

Bias winding is employed to produce the bias voltage required to energize the controller circuits. This voltage is maintained at a greater level than the start-up circuit voltage to ensure that a PWM controller circuit draws current from the bias winding rather than the start-up circuit. The current Transformer senses the Input current and protects the converter from overcurrent and short circuit current. For the controlling Switch in the Input side of the forward Converter because of variation in Input power supply from 34V-44V. Another name for a Mag-Amp is a saturable inductor. The typical Transformer and Inductor have ferrite-based high-impedance cores, which must not reach saturation as their primary function in the circuit is energy transfer. Mag-Amp is employed in circuits as a switch. It should exhibit high impedance while not saturated and zero impedance when saturated, like an ideal switch.

4. SPECIFICATION AND DESIGN DETAILS

The design specifications of the proposed Forward Converter are shown in Table 1.

Table 1 Specification of the Converter

CONVERTER SPECIFICATION	
Minimum input voltage	28 V
Maximum input voltage	44 V
Output voltage (Vout1, Vout2)	+8.2 V, -8.2V
Output current (Iout1, Iout2)	5.7A, 0.5A
Switching frequency	140 KHz
Maximum duty cycle	40%
Efficiency	70 %
Line Regulation	<1%
Load Regulation	<1%
Time Period	7.14usec
Operating Temperature Range	–55°C to 125°C

4.1. Transformer Core Selection

The optimum design is decided by the small size and lower dissipation of transformer, so Window Factor (Kw), Flux Density (Bm) & Current Density (J) values are assumed, for optimal designing by preventing hazardous voltage contact

$$Ap = Ac \,\square\, Aw \tag{1}$$

$$Ap = \frac{\sqrt{Dmax} \times Pout \times (1 + \frac{1}{Eff})}{Kw \times J \times 10^{-6} \times Bm \times Fsw} \tag{2}$$

Turns Ratio

$$N_p = \frac{(V_{in_{min}} * D_{max})}{B_m * A_c * 10^{-6} * F_{sw}} \tag{3}$$

$$T_{ratio} = \frac{N_s}{N_p} = \frac{V_{out} + (V_D * D_{max})}{D_{max} * V_{in_{min}}} \tag{4}$$

$$N_s = T_{ratio} * N_p \tag{5}$$

Core selected is 0R43019UG, material, Ur:5010, AL: 6680mH/1000T

Magnetic Amplifier core selection using

$$A_{P_{MA}} = \frac{A_X * V_{withstand}}{B * K_F * 10^{-6}} \tag{6}$$

Selected core is P/N: 6-L2016-W763 (Nanocrystalline MagAmp Cores)

4.2. Selection of MOSFET switch

The choice of MOSFET is contingent upon several factors, including the Drain-Source voltage (VDS), Drain current (Id), Drain-Source ON resistance (Rds_on), Gate charge (Qg), and Output Capacitance (Coss). The selection and dimensions of a MOSFET are determined by the losses that occur within it.

$$V_{peak_{MOSFET}} = V_{in_{max}} * \left(1 + \frac{N_p}{N_{mag}}\right) \tag{7}$$

IRHM57260, 200V, 0.049 Ohm, 32@ 100 Deg has been selected.

4.3. Output Filter

The secondary output voltage of Transformers is rectified and filtered in order to achieve the desired output parameters. The proposed converter utilizes an LC filter, and it is crucial to select the optimal values for this filter. This ensures that the converters have minimal noise, are compact, and cost-effective, which are the primary requirements for Space applications.

$$L = \frac{V_{out_s} * (1 - D_{min_s}) * T_s}{2 * \Delta I_L} \tag{8}$$

$$C = \frac{(1 - D_{min_s}) * I_{out_s}}{8 * L * F_{sw}^2 * V_{D_{Delta}}} \tag{9}$$

4.4. Secondary Diode Selection

The selection of the output diode is contingent upon the magnitude of the secondary current and voltage. The essential requirement for these diodes is that they must operate at high frequencies. During the transition from the ON state to the OFF state, the reverse recovery time of a standard signal or p-n diode typically ranges in the order of hundreds of nanoseconds. However, for fast recovery diodes, this period is less than 100 nanoseconds. On the other hand, Schottky diodes have an extremely low reverse recovery time, almost nil. Schottky diodes are very appropriate due to their minimal forward voltage drop (VFD), high current capacity (IF), and low reverse recovery time (Trr)

Selected diode is 35CGQ100, 100V, 35A, TO-254AA, V_{FD}: 0. 6.

5. HARDWARE IMPLEMENTATION

The converter is activated by a direct current (DC) voltage source and its output is linked to an electronic load that measures the output voltage and load current. A digital storage oscilloscope (DSO) is connected to measure the ripple in the outputs.

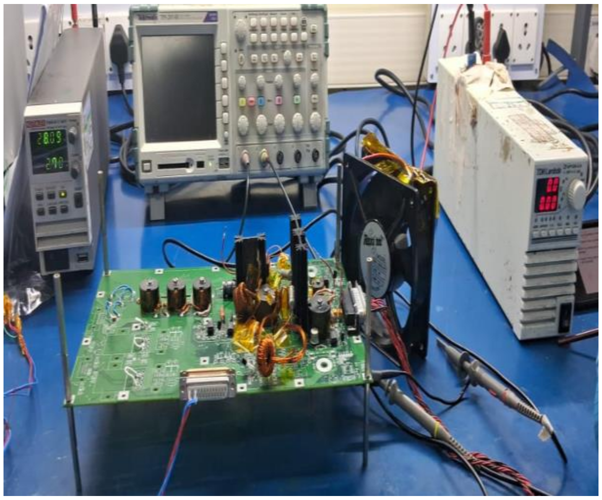

Fig. 4. Hardware Setup

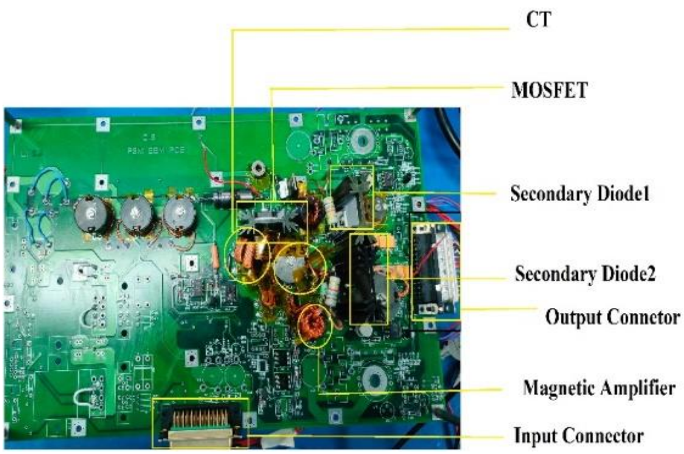

Fig. 5. Top View

Fig. 6. Bottom View

Fig 5 The hardware setup includes a Hardware Board, a Multimeter for measuring Voltage and current, a DC Supply for providing input voltage to the converter, a CRO for measuring and capturing the waveform, and an Electronic Load for measuring the output voltage and current.

6. RESULTS AND DISCUSSION

Hardware results for the converter at various load condition and input voltage are discussed below.

6.1. MOSFET

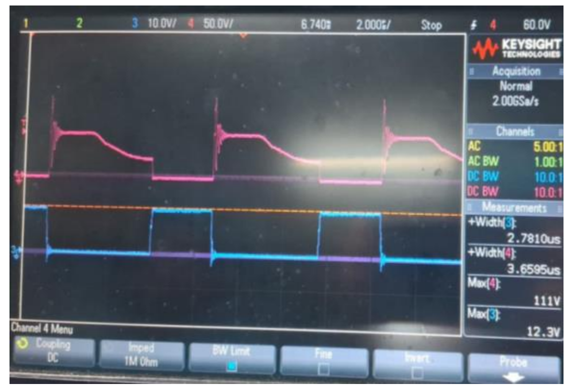

Fig. 7. Vgs and Vds at 34V

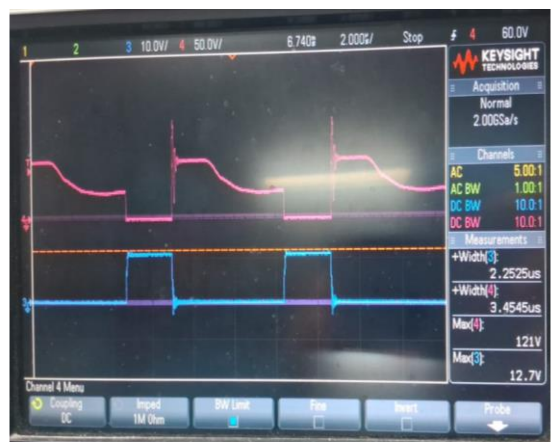

Fig. 8. Vgs and Vds at 38V

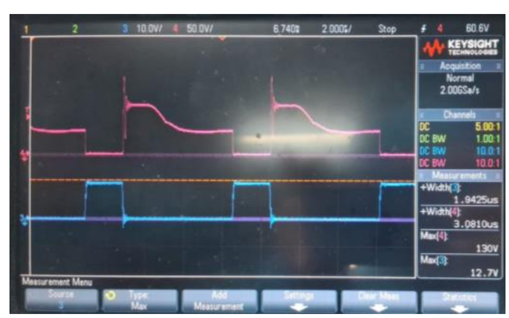

Fig. 9. Vgs and Vds at 43V

Table shows the MOSFT Vgs, Vds and Duty cycle Readings for a Various Input Voltage

Table 2 Vgs, Vds and Duty at various input voltage

Input Voltage (V)	At Minimum Load (10%)	At Half Load (50%)	At Full Load (100%)	At Minimum Load (10%)	At Half Load (50%)	At Full Load (100%)
34	24.4mV	18.6mV	13.8mV	23.4mV	16mV	17.8mV
38	18.8mV	13.8mV	14.6mV	18.8mV	13.8mV	16.6mV
43	19.2mV	18mV	18mV	19.2mV	18mV	18mV

6.2. Mag-Amp Output

MAG-AMP Voltage Waveform output 1 at Full load condition. Fig 10, Fig 11 and Fig 12 shows Voltage across Mag-Amp at 34V, 38V and 43V input voltages respectively measured at Full load current (5.7A) conditions.

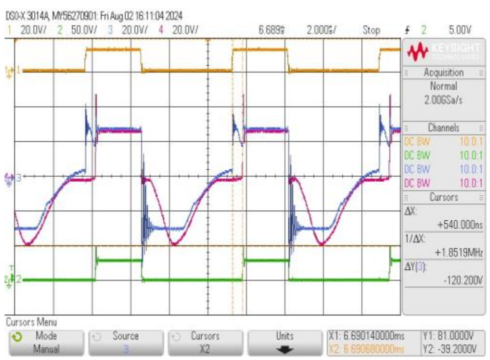

Fig. 10. Mag-Amp Output 1 at 34V

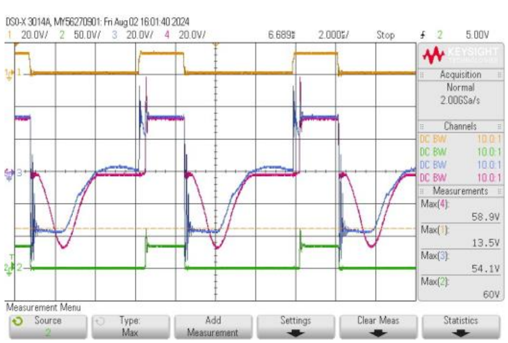

Fig. 11. Mag-Amp Output 1 at 38V

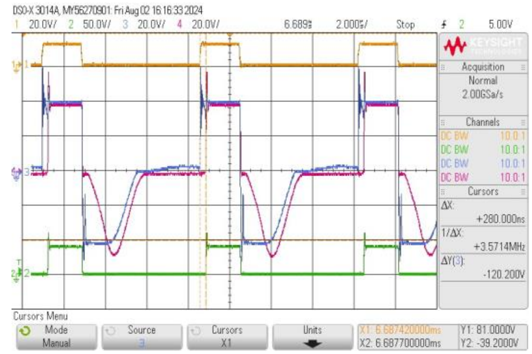

Fig. 12. Mag-Amp Output 1 at 43V

Table shows the Mag-Amp Blocking time at various input voltage and load condition

Table 3 Mag- Amp blocking time

Input Voltage (V)	Input Current (A)	Gate to Source Voltage (Vgs)	Drain to Source Voltage (Vds)	Measured Value
34V	1.82	12.5V	122V	0.28
38V	1.68	12.5V	124V	0.37
43V	1.5	12.9V	132V	0.32

6.3. Efficiency at Full load

Table 4 shows the Output transformer voltage, Drain Voltage, Ripple voltage, Output Voltage, and Efficiency calculated at various Voltages. From the table, it is observed that at maximum Efficiency is achieved at 34V. The overall Efficiency of the converter is >70% is achieved as the specified value.

Table 4 Efficiency calculation at various voltage

in/p v/g	in/p current	O/p tra v/g	Drain voltage	o/p 1 v/g	o/p 2 v/g	ripple v/g (mV)	Effiy(%)
38	1.73	52.8	64.5	8.212	8.269	17.6	81.2
43	1.53	66	104	8.213	8.268	18.4	81.185
34	1.93	48	120	8.214	8.269	16	81.40
30	2.24	44	112	8.215	8.27	16.6	79.50
28	2.41	43	108	8.214	8.27	19	79.162

6.4. Output Ripple Voltage

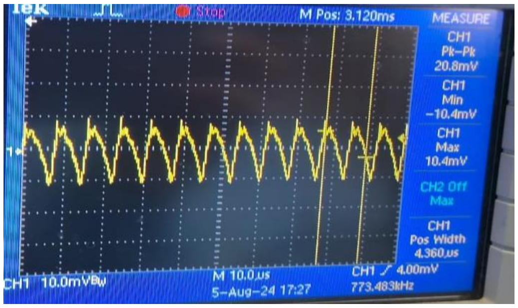

Fig. 11. Output 1 ripple at 38V

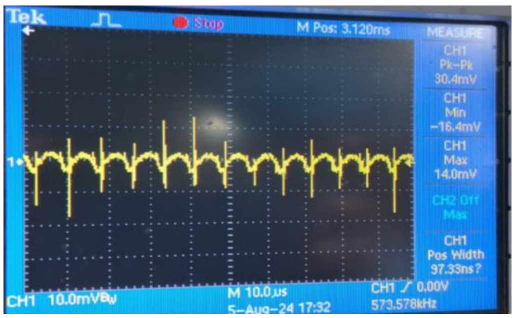

Fig. 12. Output 2 ripple at 38V

Table 5 shows the output 1 ripple voltage at various voltages.

Table 5 Mag- Amp blocking time

Input Voltage (V)	At Minimum Load (10%)	At Half Load (50%)	At Full Load (100%)
34	27.4mV	21.6mV	15.8mV
38	18.8mV	13.8mV	14.6mV
43	19.2mV	18mV	18mV

6.5. Line and Load Regulation

Table 6 shows the line and load regulation at various input voltage and load condition

Table 6 Line and load regulation

Load	Output Voltage [+Vout (+8.2Volts)]			Output Voltage [+Vout (-8.2Volts)]			Line Regulation
	Vin=34 V	Vin=38 V	Vin=43 V	Vin=34 V	Vin=38 V	Vin=43 V	
100% (2A)	8.201	8.202	8.202	8.265	8.266	8.265	0.01
50% (1A)	8.223	8.223	8.223	8.268	8.268	8.268	
10% (0.2A)	8.238	8.239	8.23	8.27	8.27	8.26	
%load regulation	0.44			0.06			

7. CONCLUSION

Line and Load regulations met the required standards and were comfortably within 1% (0.44% and 0.06% respectively).

The output voltage exhibits a maximum change of 5% while the input voltage ranges from 34V to 44V. The converter's efficiency exceeds the specified value of 70% and is deemed satisfactory according to the specifications. Hence, the Power Supply is specifically built to meet special needs and is well-suited for use in Space applications.

REFERENCES

[1] X. Xiong, X. Ruan, H. Xi and J. Ge, "Feed-Forwarding the Output Voltage to Improve Efficiency for Envelope-Tracking Power Supply Based on a Switch-Linear Hybrid Scheme," in *IEEE Transactions on Power Electronics*, vol. 26, no. 8, pp. 2106-2111, Aug. 2011, doi: 10.1109/TPEL.2011.2119494.

[2] Suresh Kumar Tummala, Lenine Duraiswamy, "Switched Mode Power Supply: A High Efficient Low Noise Forward Converter Design Topology", 2022 IEEE 2nd International Conference on Sustainable Energy and Future Electric Transportation (SeFeT), Hyderabad, India (2022), August 04-06. Doi: 10.1109/SeFeT55524.2022.9908809.

[3] Nesh J, Bhoopendra Kumar Singh et.al, "Overview of Space Grade Power Supply Modules for Satellite", Edited by PSR Srinivasa Sastry, Jiji CV et.al, Advances in Small Satellite Technologies, Lecture Notes in Mechanical Engineering. Springer, Singapore, May (2020), pp. 257-271. Doi: 10.1007/978-981-15-1724-2_27.

[4] Gerry Moschopoulos, IEEE Press Editorial Board Sarah Spurgeon, Editor in Chief, "DC-DC Converter Topologies: Basic to Advanced", Wiley-IEEE Press, New Jersey, (2024).

[4] Soumya K, Arpitha Raju B et.al, "Single Output 40W DC-DC Forward Converter for Space Application", International Research Journal of Engineering and Technology, vol. 09, Issue.05, May (2022), pp. 3165-3173.

[5] Guthi Prakash, Santosh B L and Bhoopendra Kumar Singh, "Spaceborne forward converter with discrete LDO to power OCXO", 2020 International Conference on Smart Technologies in Computing, Electrical and Electronics (ICSTCEE), Bengaluru, India (2020), December 09-10, Doi: 10.1109/ICSTCEE49637.2020.9276812.

[6] A. Bhat, K. U. Rao, Praveen P K, B. K. Singh and V. Chippalkatti, "Multiple output forward DC-DC converter with Mag-amp post regulators and voltage feedforward control for space application", 2016 Biennial International Conference on Power and Energy Systems: Towards Sustainable Energy (PESTSE), (2016), pp. 1-6, doi: 10.1109/PESTSE.2016.7516488.

[7] Abraham I, Pressman et.al, Wendy Rinaldi- Sponsoring Editor, “Switching power supply design”, Third Edition, McGraw-Hill Publication, New York, (2009).

[8] Xu Congwen, Ma Qishuang et.al, “Closed-Loop Gate Drive for Single-Ended Forward Converter to Reduce Conducted EMI”, IEEE Access, Vol. 8, June (2020), PP (99):1-1, Doi: 10.1109/ACCESS.2020.3005239

[9] Soumya Patil, R.S. Geetha et.al, “Design and implementation of multiple output forward converter with Mag-Amp and LDO as post regulators for space application”, International Journal of Engineering Science and Technology, vol. 12, Issue.03, May (2020), pp. 43-56., DOI:10.4314/ijest. v12i3.5.

[10] Hesamodin Allahyari, Mohammad Ali Latifzadeh et.al, “An Improved Single Switch Wide Range ZVS Forward Converter Controlled with Variable Magnetizing Inductance”, IEEE Journal of Emerging and Selected Topics in Industrial Electronics, vol. 5, Issue.3, July (2024), pp. 837- 847. Doi:10.1109/JESTIE.2023.3311170.

[11] Jennifer Ian G. Ligtao, Chinet M. et.al, “Implementation of On-chip OVP, OCP and OTP Circuits for DC-DC Converter Design”, 2018 IEEE 10th International Conference on Humanoid, Nanotechnology, Information Technology, Communication and Control, Environment and Management (HNICEM), Baguio City, Philippines (2018), November 29- December 02. Doi: 10.1109/HNICEM.2018.8666254.

[12] S. Kuruva, C. G. Satyaraddi et.al, "Design and Implementation of Multiple Output DC-DC Converter with Output Power Sequencing", 2021 6th International Conference for Convergence in Technology (I2CT), Maharashtra, India (2021), April 02-04, Doi: 10.1109/I2CT51068.2021.9417822.